R. & M. No. 3146
(20,597)
A.R.C. Technical Report

R. & M. No. 3146

MINISTRY OF AVIATION

AERONAUTICAL RESEARCH COUNCIL
REPORTS AND MEMORANDA

# A Method of Calculating the Velocity Distribution on Annular Aerofoils in Incompressible Flow

By J. A. Bagley, B.Sc., N. B. Kirby and P. J. Marcer

LONDON: HER MAJESTY'S STATIONERY OFFICE
1961
NINE SHILLINGS NET

# A Method of Calculating the Velocity Distribution on Annular Aerofoils in Incompressible Flow

By J. A. Bagley, B.Sc., N. B. Kirby and P. J. Marcer*

Communicated by the Director-General of Scientific Research (Air), Ministry of Supply

*Reports and Memoranda No. 3146†*
*June, 1958*

*Summary.*—A method of calculating the velocity distribution in incompressible flow on annular aerofoils of moderate thickness/chord ratio and camber, and reasonably large radius/chord ratio (the order of 1 or greater), is developed, based on the use of distributions of singularities on a cylinder whose velocity fields are tabulated here and in Ref. 1.

The annular wing at zero incidence is treated first, and then the wing at incidence. Examples of the calculated velocity distributions on various aerofoils are given.

1. *Introduction.*—Annular aerofoils are cylindrical fairings whose streamwise section is an aerofoil profile; they can be used as fairings for various types of propulsive systems, *e.g.*, propellers and turbojet engines. Their usual function is to increase the efficiency of such systems by increasing the mass flow through the system for a given power input. Other designs of annular fairings can be used to alleviate compressibility effects. A survey of some possible applications has been given in Chapter 6 of Ref. 1.

Until recently, there have been few practical applications of such installations in aeronautics, but serious work has been done in the last few years on aircraft with annular wings, especially for 'vertical take-off' applications; in France, Zborowski and the S.N.E.C.M.A. concern have developed such designs under the name 'coleopter'[2]. Ducted propellers have been used as the lift-producing system on several American designs such as the Hiller VZ–1E, Piasecki 59K, and Doak 16. Some typical applications of annular wings are shown in Fig. 1.

No simple method of calculating the velocity distribution on annular wings of finite thickness appeared to be available when the present work was initiated in 1955‡. The infinitely thin cambered annular aerofoil at zero incidence has been treated by Küchemann and Weber (Ref. 1, Section 5.4);

* The bulk of the work in this paper was done by P. J. Marcer, of Liverpool University, and N. B. Kirby, of the Royal Military College of Science, Shrivenham, while working as vacation students at the Royal Aircraft Establishment during July/August, 1955, and July/August, 1957, respectively.

† R.A.E. Tech. Note Aero. 2571, received 3rd December, 1958.

‡ Since the completion of the work described in this paper, a further report by Weissinger[11] has become available, in which he has extended his earlier work[5] to enable surface velocity distributions to be calculated, in a similar way to that presented in Section 3 here.

and Ribner[3], Faure[4] and Weissinger[5] have calculated the overall aerodynamic forces on an infinitely thin annular aerofoil at incidence in incompressible flow. Weissinger's work[5] can be developed to give the velocity distribution on the aerofoil, and this is done in Section 3 of the present note. Calculations on annular aerofoils have also been made using the electrolytic-tank analogy: Malavard[6] has summarised recent French work. Hacques[10] has used this method to find the aerofoil section shape which, on an annular aerofoil, has the same pressure distribution at zero incidence as a biconvex parabolic arc section has in two-dimensional flow, but the inverse problem of calculating the pressures on a given annular aerofoil has apparently not been tackled.

In the present report, a method is developed which enables the velocity distribution to be calculated on annular aerofoils with moderate thickness/chord ratios and radius/chord ratios of the order of unity or larger in incompressible, non-viscous flow. This method uses distributions of singularities on a cylinder, whose strengths can easily be determined from the geometry of the system, and whose velocity fields are tabulated here or in other papers. The results for some typical examples are given.

2. *Annular Aerofoils at Zero Incidence.* 2.1. *Thin Aerofoils.* The calculation method for thick aerofoils developed in this note is based upon the Küchemann-Weber method for thin aerofoils[1], which will first be recapitulated.

The flow about a thin annular aerofoil at zero incidence can be represented by the velocity field of a distribution of bound vortices on the aerofoil. For small values of local surface slope (*i.e.*, camber or conicity), and for values of the radius/chord ratio greater than about 1/4, it is adequate to place the singularities on a mean cylinder of constant radius, and to calculate the velocities induced by the vortices at points on this cylinder, instead of on the aerofoil surface itself.

If $v_x(x, r)$ and $v_r(x, r)$ are the streamwise and radial velocity increments due to the distribution of bound vortices, they are related to the aerofoil shape $r(x)$ by the streamline condition:

$$\frac{dr}{dx} = \frac{v_r(x, r)}{V_0 + v_x(x, r)} . \tag{1}$$

This equation forms the basis from which the two main problems may be solved: (*a*) to find the velocity distribution on an aerofoil of given shape and (*b*) to calculate the shape needed to give a particular velocity distribution. Only the first problem is considered in this report.

The simplest method of dealing with equation (1) numerically is to make use of a series of standard vortex distributions whose velocity fields have been tabulated. In the Appendix of Ref. 1, the velocity fields of five vortex distributions* placed on cylinders of various radius/chord ratios have been tabulated. By using these Tables, equation (1) can be satisfied at up to five points, giving five simultaneous equations from which the strength of the five standard distributions can be found, and enabling the velocity distribution on the surface of the cylinder to be calculated.

---

* These comprise the first three distributions of the Birnbaum series, *viz.*,

$$\gamma_1(x) = 2\pi V_0 \sqrt{\left(\frac{1 - x}{x}\right)}$$

$$\gamma_2(x) = 2\pi V_0 \sqrt{\{1 - (1 - 2x)^2\}}$$

$$\gamma_3(x) = 2\pi V_0(1 - 2x) \sqrt{\{1 - (1 - 2x)^2\}}$$

and the constant and linear distributions, $\gamma_4 = 2\pi V_0$ and $\gamma_5 = 2\pi V_0(1 - 2x)$.

2.2. *Aerofoils of Finite Thickness.* Just as the theory of two-dimensional thick aerofoils can be developed from that of thin aerofoils by the addition of a source-sink distribution on the aerofoil surface (which can usually be approximated by a distribution along the chord-line), so the annular aerofoil of finite thickness will here be represented by the addition of a source distribution to the vortex distribution considered in Section 2.1.

In the two-dimensional case, the condition that the aerofoil surface $z = z_t(x)$ is a streamline is

$$\frac{dz_t}{dx} = \frac{v_z(x, z)}{V_0 + v_x(x, z)}.$$

If the aerofoil is reasonably thin, this can be simplified by assuming that $v_x$ is small compared with $V_0$, and that $v_z(x, z)$ on the surface can be approximated by $v_z(x, 0)$ on the chord-line. Since, for a plane source distribution, the value of $v_z(x, 0)$ depends only on the local source strength $q(x)$, the streamline condition becomes

$$\frac{dz_t}{dx} = \frac{v_z(x, 0)}{V_0} = \frac{q(x)}{2V_0},$$

i.e.,

$$q(x) = 2V_0 \frac{dz_t}{dx}. \tag{2}$$

The velocity distribution around the aerofoil has then been shown by Weber[7] to be approximately

$$\frac{V}{V_0} = \frac{1 + \frac{1}{\pi}\int_0^1 \left(\frac{dz_t}{dx}\right)_{x=x'} \frac{dx'}{x - x'}}{\sqrt{\left\{1 + \left(\frac{dz_t}{dx}\right)^2\right\}}},$$

which can conveniently be written

$$\frac{V}{V_0} = \frac{1 + S^{(1)}(x)}{\sqrt{[1 + \{S^{(2)}(x)\}^2]}},$$

where

$$S^{(1)}(x_\nu) = \frac{1}{\pi}\int_0^1 \left(\frac{dz_t}{dx}\right)_{x=x'} \frac{dx'}{x_\nu - x'} = \sum_{\mu=1}^{N-1} s_{\mu\nu}^{(1)} z_t(x_\mu)$$

and

$$S^{(2)}(x_\nu) = \left(\frac{dz_t}{dx}\right)_{x=x_\nu} = \sum_{\mu=1}^{N-1} s_{\mu\nu}^{(2)} z_t(x_\mu)$$

are sum-functions of the aerofoil ordinates at certain specified stations $x_\mu$. The coefficients $s_{\mu\nu}^{(1)}$ and $s_{\mu\nu}^{(2)}$ are tabulated in Ref. 7.

In dealing with the annular aerofoil, it is convenient to consider a source distribution on the mean cylinder, and to calculate the velocities on this cylinder instead of at the aerofoil surface. Equation (2) connecting the source strength and the aerofoil thickness distribution can then be retained, as is shown in Appendix I, but this source distribution placed on a cylinder gives a distribution of radial velocities which includes a term depending on the whole source distribution, additional to that depending only on the local source strength. (The expressions for the axial and radial velocities due to the distribution of sources on the cylinder are given in Appendix I.) This additional term represents a curvature of the flow past the source distribution, and can be considered

as an effective camber of the aerofoil section. To represent an uncambered section thus requires the addition of a vortex distribution to the source distribution.

Equation (1) is thus replaced, for the thick aerofoil, by the equation

$$\frac{v_{qr} + v_{\gamma r}}{V_0 + v_{qx} + v_{\gamma x}} = \frac{dr}{dx}, \tag{3}$$

where $v_{\gamma x}$ and $v_{\gamma r}$ are the axial and radial velocity components due to the vortex distribution, $v_{qx}$ and $v_{qr}$ are the axial and radial† velocity components due to the source distribution, and $(dr/dx)$ is the slope of the skeleton line of the aerofoil.

For the range of section thicknesses and radius/chord ratios considered here, it will be adequate to assume that $(v_{qx} + v_{\gamma x})$ is small compared with $V_0$, and to replace equation (3) by the linearised form

$$\frac{v_{qr} + v_{\gamma r}}{V_0} = \frac{dr}{dx}. \tag{4}$$

$v_{qr}/V_0$ can be calculated from the known source distribution (*see* Appendix I, or equation (8) below) and $dr/dx$ is known, so equation (4) can be satisfied at five (or fewer) points along the aerofoil chord by using the tabulated velocity fields of the five standard vortex distributions in the Appendix of Ref. 1.

This gives

$$\frac{v_{\gamma r}(x)}{V_0} = \sum_{m=1}^{5} C_m v_{rm}^{*}(x), \tag{5}$$

where $v_{rm}^{*}(x)$ are tabulated, so that the coefficients $C_m$ can be found. The axial velocity increment due to the effective camber is then

$$\frac{v_{\gamma x}(x)}{V_0} = \sum_{m=1}^{5} C_m v_{xm}^{*}(x) \pm \sum_{m=1}^{5} \frac{C_m \gamma_m}{2V_0}, \tag{6}$$

where the $v_{xm}^{*}(x)$ are also tabulated in Ref. 1, and with the sign convention used there the positive sign in (7) is to be taken on the inner surface of the aerofoil and the negative sign on the outer surface.

In Appendix I, the velocities on the cylinder due to the source distribution are derived in the form:

$$\begin{aligned}\frac{v_{qx}(x_\nu)}{V_0} &= S^{(1)}(x_\nu) + S^{(27)}(x_\nu) \\ &= \sum_{\mu=1}^{N-1} s_{\mu\nu}^{(1)} z_t(x_\mu) + \sum_{\mu=1}^{N-1} s_{\mu\nu}^{(27)} z_t(x_\mu)\end{aligned} \tag{7}$$

$$\begin{aligned}\frac{v_{qr}(x_\nu)}{V_0} &= S^{(28)}(x_\nu) \pm \left(\frac{dz_t}{dx}\right)_{x_\nu} \\ &= \sum_{\mu=1}^{N-1} s_{\mu\nu}^{(28)} z_t(x_\mu) \pm \left(\frac{dz_t}{dx}\right)_{x_\nu},\end{aligned} \tag{8}$$

† $v_{qr}$ in equation (3) omits the term $\pm \frac{1}{2}q(x) = \pm (dz_t/dx)$.

where the coefficients $s_{\mu\nu}^{(27)}$ and $s_{\mu\nu}^{(28)}$ are given in Tables 1 and 2. The fixed positions $x_\mu$ are the same as occur in Ref. 7; they are also tabulated in Table 3 of this report.

The total axial velocity on the annular aerofoil at zero incidence is then given by

$$V = V_0 + v_{qx} + v_{\gamma x}\,, \tag{9}$$

where $v_{qx}$ and $v_{\gamma x}$ are to be taken from equations (7) and (6) respectively.

In dealing with the two-dimensional symmetrical aerofoil Weber[7] has shown that the velocity on the aerofoil surface is obtained approximately from that calculated at the chord-line by multiplying the latter by the factor $\{1 + (dz/dx)^2\}^{-1/2}$, and a considerable improvement in the linearised theory is thus obtained. The same factor will therefore be applied here to the total velocity given by equation (9), so that the final expression for the velocity on the surface of the annular aerofoil becomes

$$\frac{V}{V_0} = \frac{1}{\{1 + (dz/dx)^2\}^{1/2}}\left[1 + \sum_{\mu=1}^{N-1} s_{\mu\nu}^{(1)}\, z_t(x_\mu) + \sum_{\mu=1}^{N-1} s_{\mu\nu}^{(27)}\, z_t(x_\mu) + \right.$$
$$\left. + \sum_{m=1}^{5} C_m\, v_{xm}^{*} \pm \sum_{m=1}^{5} C_m \frac{\gamma_m}{2V_0}\right]. \tag{10}$$

A minor practical inconvenience arises in using equation (10), since the value of $v_{qx}$ is obtained at the special stations $x = x_\nu$, while the tables in Ref. 1 give the values of $v_{\gamma x}$ at the stations $x = 0$, 0·05, 0·1, 0·15 . . . . etc. It is thus necessary to interpolate values of one or other term by graphical or similar means.

2.3. *Calculated Examples.* The method outlined in Section 2.2 has been applied to four typical examples. The first two have RAE 101 symmetrical sections with a thickness/chord ratio of 10 per cent, and radius/chord ratios of $\frac{1}{2}$ and 1 respectively.

For these symmetrical sections, equation (4) reduces to

$$\frac{v_{\gamma r}}{V_0} = -\frac{v_{qr}}{V_0}\,. \tag{11}$$

In Fig. 2, $v_{qr}/V_0$ (less the term $\pm\, q/2V_0$) calculated from equation (8) for the case $R = 1$ is compared with two versions of $v_{\gamma r}/V_0$ from equation (5), using 5 and 3 standard vortex distributions respectively. As can be seen, the increase in the number of distributions used does not greatly increase the accuracy with which equation (11) is satisfied, and in fact the introduction of $\gamma_4$ and $\gamma_5$ leads to the appearance of an infinite radial velocity at both the leading and trailing edges. The comparison between the axial velocities calculated by using the three-term and five-term versions of equation (6) is given in Fig. 3, and the difference between them (except near $x = 0$) is insignificant.

From this, it appears that it should be sufficient in practice to use only the first three standard vortex distributions, and in the subsequent examples, this has been done.

In Fig. 4, the contributions of the various terms in equation (9) are shown, for the case $R = \frac{1}{2}$. It appears that the 'direct' effect of the source distribution is virtually identical with the two-dimensional case, the term $S^{(27)}(x)$ being negligible. The 'induced camber' effect, measured by the terms $\Sigma\, C_m v_{xm}^{*}$ and $\Sigma\, C_m(\gamma_m/2V_0)$, is the important one. It should be noted that higher velocities are induced on the inner surface of the annular wing than on the outer surface, so that a radial force acting inwards is produced.

Fig. 5 shows the final result obtained from equation (10) for the cases $R = \frac{1}{2}$ and $R = 1$, compared with the two-dimensional result, $R = \infty$. It is clear that the pressure distribution on the outside of the aerofoil does not change very much with decreasing radius/chord ratio; on the inside the changes produced are greater.

As a further example of the calculation method, pressure distributions have been calculated, for $R = \frac{1}{2}$ and $R = 1$, on annular aerofoils with a cambered basic section. The section chosen has a 10 per cent RAE 101 thickness distribution, superimposed on a 5 per cent RAE 101 mean line. This shape would have a flat inner surface (although the shape close to the nose would probably have to be modified somewhat in any practical case). The results are shown in Fig. 6.

3. *Annular Aerofoils at Incidence.* It will be assumed that the velocity increments due to incidence and those due to thickness can be linearly superposed. This Section thus deals with a circular cylinder of zero thickness which is placed in a uniform stream inclined at an angle $\alpha$ to the axis of the cylinder. The results of Section 2 can then be added to this to give the velocity distribution at incidence on an annular aerofoil of finite thickness and camber.

If the boundary condition that the cylinder is a stream-surface of the flow is also linearised, then the vertical velocity component, $v_z$, at any point $(x, R, \varphi)$ of the aerofoil is constant, equal to $-V_0 \tan \alpha$. This implies that the radial velocity component

$$\frac{v_r}{V_0}(x, R, \varphi) = \frac{v_z}{V_0} \cos \varphi = -\tan \alpha \quad \cos \varphi \tag{12}$$

(taking $\varphi = 0$ at the 'top' of the aerofoil).

Weissinger[5] has shown that distributions of bound vortex rings with the local strength

$$\gamma(x, \varphi) = V_0 \sum_{n=0}^{\infty} g_n(x) \cos n\varphi ,$$

together with the corresponding trailing vortices (of strength $1/R \cdot d\gamma/d\varphi$) on a cylinder of radius $R$, can be used to satisfy the boundary condition

$$\frac{v_r}{V_0} = \sum_{n=0}^{\infty} \alpha_n(x) \cos n\varphi .$$

For the case which is of interest here, namely, $n = 1$, Weissinger has solved this problem by taking a Birnbaum series for $g_1(x)$:

$$g_1(x) = A_1 2\pi \sqrt{\left(\frac{1-x}{x}\right)} + A_2 2\pi \sqrt{\{1 - (1-2x)^2\}} +$$

$$+ A_3 2\pi(1-2x) \sqrt{\{1 - (1-2x)^2\}} + \ldots \quad . \tag{13}$$

For the case $\alpha(x)$ = constant, values of the coefficients $A_1$, $A_2$, $A_3$ for various values of the radius/chord ratio obtained from Weissinger's work[5] are given in the following Table†:

| $R$ | $A_1/\tan\alpha$ | $A_2/\tan\alpha$ | $A_3/\tan\alpha$ |
|---|---|---|---|
| 1/4 | −0·0896 | +0·0797 | +0·0530 |
| 1/3 | −0·1036 | +0·0768 | +0·0391 |
| 1/2 | −0·1266 | +0·0661 | +0·0216 |
| 1 | −0·1747 | +0·0379 | +0·0056 |
| ∞ | $-1/\pi = -0{\cdot}3183$ | 0 | 0 |

The axial velocity distributions at points on the cylinder induced by these Birnbaum vortices are calculated in Appendix II of this paper. It may be noted that only the bound vortex elements will give an axial velocity component. To calculate the surface pressure distributions, the circumferential velocity components $v_\varphi$ induced by both the bound and trailing vortices would have to be included, although for small incidences this contribution can be ignored since it is proportional to the square of the incidence.

The axial velocity increment due to incidence is thus

$$\left(\sum_{m=1}^{3} A_m v_{xm}^{**} \pm \sum_{m=1}^{3} A_m \frac{\gamma_m}{2V_0}\right) \cos\varphi\,, \tag{14}$$

where the positive sign in this convention refers to the inner surface and the negative sign to the outer surface. The final expression for the velocity on the surface of a thick annular aerofoil at incidence is obtained by adding these terms to equation (10):

$$\frac{V}{V_0} = \frac{1}{\{1 + (dz_t/dx)^2\}^{1/2}} \left[1 + \sum_{\mu=1}^{N-1} (s_{\mu\nu}^{(1)} + s^{(27)}_{\mu\nu})\, z_t(x_\mu) + \right.$$
$$+ \sum_{m=1}^{5} C_m v_{xm}^{*} \pm \sum_{m=1}^{5} C_m \frac{\gamma_m}{2V_0} +$$
$$\left. + \cos\varphi \left(\sum_{m=1}^{3} A_m v_{xm}^{**} \pm \sum_{m=1}^{3} A_m \frac{\gamma_m}{2V_0}\right)\right]. \tag{15}$$

Equation (15) has been used to calculate the velocity distribution on the 10 per cent thick RAE 101 uncambered aerofoil with radius/chord ratio of unity at $\alpha = 5$ deg, and the result is shown in Fig. 7. The velocities on the inner and outer surfaces at $\varphi = 0$ deg and 180 deg (the top and bottom of the aerofoil) are shown. The most significant feature of the results is the marked asymmetry in the velocity distribution between the top and bottom halves of the aerofoil: clearly the lower part contributes the bigger part of the total lift force.

---

† In Weissinger's report[5], coefficients $C_0 = -2\pi A_1$, $C_1 = -2\pi A_2$ and $C_2 = -\pi A_3$ are used; a different nomenclature has been used here to preserve consistency with Ref. 1. In Ref. 5, values of the coefficients $C_3$ and $C_4$ of higher terms in the series are also given for the cases $R = 1/4$ and $R = 1/10$. It must also be observed that in the present report, following the usage of Ref. 1, vortices are counted positive which rotate anti-clockwise in a system where $x$ (and $V_0$) are positive to the right so that a positive circulation leads to increased mass flow through the wing; this is in the contrary sense to the convention normally used in two-dimensional aerofoil theory, and also by Weissinger in Ref. 5.

4. *Conclusions.* In this report, a method has been developed which enables the velocity distribution to be calculated on the surface of a moderately thick annular aerofoil. This should be useful as a tool in designing such aerofoils, and as an aid to understanding the causes of flow separations which may occur in a viscous flow. It is believed that one of the major reasons for the lack of success obtained by many experimenters on ducted airscrews in the past has been the occurrence of large flow separations on the annular fairing, most frequently near the leading edge or due to large adverse pressure gradients near the trailing edge. The existence of a suitable design method for predicting pressure distributions should help to overcome this difficulty.

The work described here is only a contribution towards the complete theory which is needed; an isolated annular aerofoil will never occur in practice, but will contain a central body, or an airscrew, or a jet engine. In principle, these can be dealt with by adding further distributions of singularities to the flow. For example, the central body can be represented by a distribution of sources and sinks along its axis, and an airscrew can be replaced by a uniform distribution of sinks, as is shown in Ref. 1, pp. 130 to 133. To preserve the condition that the aerofoil, or its mean surface, is a stream-surface of the combined flow, the singularities representing the aerofoil have to be appropriately modified to cancel the normal velocities induced by the added singularities.

## LIST OF SYMBOLS

| | |
|---|---|
| $A_1, A_2, A_3, A_m$ | Coefficients of the vortex distributions used to represent the wing at incidence |
| $C_1, C_2, C_3, C_4, C_5, C_m$ | Coefficients of the vortex distributions used to represent the wing at zero incidence |
| $g_n(x)$ | Coefficients of vortex distributions used in Ref. 5 |
| $q$ | Source strength |
| $r$ | Radial co-ordinate |
| $R$ | Radius of aerofoil |
| $s_{\mu\nu}^{(1)}, s_{\mu\nu}^{(2)}$ | Coefficients in expressions for $S^{(1)}$, $S^{(2)}$ |
| $S^{(1)}(x) = \frac{1}{\pi}\int_0^1 \frac{dz_t}{dx}\frac{dx'}{x - x'}$ | (*See* Section 2.2) |
| $S^{(2)}(x) = \frac{dz_t}{dx}$ | (*See* Section 2.2) |
| $s_{\mu\nu}^{(27)}, s_{\mu\nu}^{(28)}$ | Coefficients in expressions for axial and radial velocities induced by source distribution on cylinder (*See* Appendix I) |
| $v_x, v_r, v_z, v_\phi$ | Velocity increments in $x$, $r$, $z$ and $\varphi$ directions |
| $v_{qx}, v_{qr}$ | Velocity increments due to sources |
| $v_{\gamma x}, v_{\gamma r}$ | Velocity increments due to vortices |
| $v_{xm}^*, v_{rm}^*$ | Axial and radial velocity increments induced by axially symmetric vortex distribution $\gamma_m$ |
| $v_{xm}^{**}, v_{rm}^{**}$ | Axial and radial velocity increments induced by vortex distribution $\gamma_m \cos\varphi$ |
| $V$ | Total velocity at point on aerofoil surface |
| $V_0$ | Free-stream velocity |
| $x$ | Axial co-ordinate: $x = 0$ at leading edge<br>$x = 1$ at trailing edge |
| $z$ | Vertical co-ordinate |
| $z_t(x)$ | Aerofoil thickness distribution |
| $\alpha$ | Incidence of aerofoil |
| $\alpha_n(x)$ | Coefficients of downwash distribution used in Ref. 5 |
| $\gamma_1, \gamma_2, \gamma_3, \gamma_4, \gamma_5, \gamma_m$ | Standard vortex distributions (defined in Section 2) |
| $\varphi$ | Angular co-ordinate; $\varphi = 0$ at top of aerofoil |

*Note.* All lengths are measured in terms of the wing chord as unit.

## LIST OF REFERENCES


| *No.* | *Author* | *Title, etc.* |
|---|---|---|
| 1 | D. Küchemann and J. Weber .. | *Aerodynamics of Propulsion.* McGraw-Hill. 1952. |
| 2 | H. V. Zborowski .. .. | The coleopter—formula for economy.<br>*Interavia.* Vol. 10. No. 1. p. 29. January, 1955 (or see *Aeroplane.* Vol. 90. p. 278, April 20, 1956).<br>Other published references have been collected by A. T. E. Bray, R.A.E. Library Bibliography 185. June, 1956. |
| 3 | H. S. Ribner .. .. .. | The ring airfoil in non-axial flow.<br>*J. Ae. Sci.* Vol. 14. p. 529. September, 1947. |
| 4 | G. Faure .. .. .. | Étude théorique de l'aile annulaire.<br>*Tech. et Sci. Aeronautiques.* Vol. 6. p. 293. 1956. |
| 5 | J. Weissinger .. .. .. | Zur Aerodynamik des Ringflügels. Die Druckverteilung dünner, fast drehsymmetrischer Flügel in Unterschallströmung.<br>D.V.L. Bericht 2, 1955; also published as Forschungsbericht 198 des Wirtschafts- und Verkehrsministeriums Nordrhein-Westfalen, 1955; also published in *Zeitschrift für Flugwissenschaften*, Vol. 4, p. 141. 1956. |
| 6 | L. C. Malavard .. .. | Recent developments in the method of the rheoelectric analogy applied to aerodynamics. Presented at I.A.S. Annual Meeting, New York, January, 1957; I.A.S. Preprint 699. |
| 7 | J. Weber .. .. .. | The calculation of the pressure distribution over the surface of two-dimensional and swept wings with symmetrical aerofoil sections.<br>R. & M. 2918. July, 1953. |
| 8 | F. Riegels .. .. .. | Formeln und Tabellen für ein in der räumlichen Potentialtheorie auftretendes elliptisches Integral.<br>*Archiv der Math.* Vol. 1. p. 117. 1949. |
| 8A | F. Riegels .. .. .. | Die Strömung um schlanke, fast drehsymmetrische Korper.<br>Mitteilungen an der Max-Planck-Institut für Strömungsforschung. No. 5. 1952.<br>Translated into English as R.A.E. Library Translation 779. October, 1958. |
| 9 | J. Weber .. .. .. | The calculation of the pressure distribution on thick wings of small aspect ratio at zero lift in subsonic flow.<br>R. & M. 2993. September, 1954. |
| 10 | G. Hacques .. .. .. | Calcul par analogie rhéoélectricque de la courbure ou de l'épaisseur d'un profil d'aile annulaire satisfaisant à une distribution de pression imposée, lorsque l'ecoulement présente la symetrie axiale.<br>*Comptes Rendus.* Vol. 245. p. 1700. November, 1957. |
| 11 | J. Weissinger .. .. .. | Zur Aerodynamik des Ringflügels.<br>III.—Der Einfluss der Profildicke.<br>D.V.L. Bericht 42. October, 1957; also published as part of Forschungsbericht 462 des Wirtschafts- und Verkehrsministerium Nordrhein-Westfalen; also published in English as: The influence of profile thickness on ring airfoils in steady incompressible flow.<br>Mitteilung 6 aus dem Institut für Angewandte Mathematik der Technische Hochschule, Karlsruhe. 1957. |

# APPENDIX I

## *The Velocity Field of a Source Distribution on a Circular Cylinder*

In the Appendix of Ref. 1, it was shown that the axial and radial velocities induced by a source distribution of strength $q(x')$ along a cylinder of unit length and radius $R$ are, at a point $(x, r)$ outside the cylinder:

$$v_{qx}(x, r) = \int_0^1 \frac{q(x')}{2\pi} \frac{2R(x - x')E(k^2)}{\{(x - x')^2 + (r - R)^2\}\sqrt{\{(x - x')^2 + (r + R)^2\}}}\, dx' \tag{16}$$

$$v_{qr}(x, r) = \int_0^1 \frac{q(x')}{2\pi} \left\{ \frac{R\{K(k^2) - E(k^2)\}}{r\sqrt{\{(x - x')^2 + (r + R)^2\}}} + \right.$$

$$\left. + \frac{2R(r - R)E(k^2)}{\{(x - x')^2 + (r - R)^2\}\sqrt{\{(x - x')^2 + (r + R)^2\}}} \right\} dx', \tag{17}$$

where $K(k^2)$ and $E(k^2)$ are the complete elliptic integrals of the first and second kinds, with the modulus

$$k^2 = \frac{4rR}{(x - x')^2 + (r + R)^2}.$$

For points on the cylinder itself, where $r = R$, the kernels of these integrals have singularities at the point $x = x'$. The integrals may be evaluated by considering the limits as $r \to R$. Thus,

$$v_{qr}(x, R) = \int_0^1 \frac{q(x')}{2\pi} \sqrt{\frac{\{K(k^2) - E(k^2)\}}{\{(x - x')^2 + 4R^2\}}}\, dx' +$$

$$+ \operatorname*{Lim}_{r \to R} \int_0^1 \frac{q(x')}{2\pi} \frac{2R(r - R)E(k^2)}{\{(x - x')^2 + (r - R)^2\}\sqrt{\{(x - x')^2 + (r + R)^2\}}}\, dx'. \tag{18}$$

The first integral still possesses a logarithmic singularity (because $K(1) \to \infty$) which is dealt with below. The second integral can be dealt with by treating separately a small region of width $2\epsilon$ across the singularity, within which mean values are taken of all the non-singular factors in the integrand. Outside this region, $r$ can be put equal to $R$, and the integrand vanishes. Thus:

$$\operatorname*{Lim}_{r \to R} \int_0^1 \frac{q(x')}{2\pi} \frac{2R(r - R)E(k^2)}{\{(x - x')^2 + (r - R)^2\}\sqrt{\{(x - x')^2 + (r + R)^2\}}}\, dx'$$

$$= \operatorname*{Lim}_{\substack{\epsilon \to 0 \\ r \to R}} \left\{ \frac{q(x)}{2\pi} \frac{2RE(0)}{2R} \int_{x-\epsilon}^{x+\epsilon} \frac{r - R}{(x - x')^2 + (r - R)^2}\, dx' \right\}$$

$$= \frac{q(x)}{2\pi} \operatorname*{Lim}_{\substack{\epsilon \to 0 \\ r \to R}} \left\{ 2(r - R) \int_0^{\epsilon} \frac{1}{(x - x')^2 + (r - R)^2}\, d(x - x') \right\}$$

$$= \frac{q(x)}{2\pi} 2 \operatorname*{Lim}_{\substack{\epsilon \to 0 \\ r \to R}} \tan^{-1}\left(\frac{\epsilon}{r - R}\right) = \pm \frac{q(x)}{2}.$$

The limit $r \to R$ is taken first.

There is thus a discontinuity in $v_{qr}$, equal to $q(x)$, as the source distribution is crossed. This is the same as the discontinuity in $v_z$ which occurs for a plane source distribution used to represent an aerofoil in two-dimensional flow. Thus the relation between the source strength and the aerofoil section shape is $q(x) = 2V_0\,(dz_t/dx)$.

Applying the same technique to equation (16) gives

$$v_{qx}(x, R) = \operatorname*{Lim}_{\varepsilon\to 0}\left\{\int_0^{x-\varepsilon} + \int_{x+\varepsilon}^1 \frac{q(x')}{2\pi}\,\frac{2RE(k^2)}{\sqrt{\{(x-x')^2+4R^2\}}}\,\frac{dx'}{(x-x')}\right\} +$$

$$+\frac{q(x)}{2\pi}\operatorname*{Lim}_{\substack{\varepsilon\to 0\\ r\to R}}\left\{\int_{x-\varepsilon}^{x+\varepsilon}\frac{x-x'}{(x-x')^2+(r-R)^2}\,dx'\right\}. \tag{19}$$

The integrand in the second term is antisymmetric about the point $x' = x$, and this term is therefore zero.

Thus, finally

$$\frac{v_{qx}(x, R)}{V_0} = \frac{1}{\pi}\int_0^1 \left(\frac{dz_t}{dx}\right)_{x=x'}\frac{2RE(k^2)}{\sqrt{\{(x-x')^2+4R^2\}}}\,\frac{dx'}{(x-x')} \tag{20}$$

$$\frac{v_{qr}(x, R)}{V_0} = \pm\left(\frac{dz_t}{dx}\right) + \frac{1}{\pi}\int_0^1 \left(\frac{dz_t}{dx}\right)_{x=x'}\frac{K(k^2)-E(k^2)}{\sqrt{\{(x-x')^2+4R^2\}}}\,dx', \tag{21}$$

where

$$k^2 = \frac{4R^2}{(x-x')^2+4R^2}.$$

The integral expressions in equations (20) and (21) are both of the form

$$\int_0^1 \left(\frac{dz_t}{dx}\right)_{x=x'} g(x')\,dx'.$$

In the Appendix of Ref. 9, Weber has shown how integrals of this type can be approximated by sum-functions of the aerofoil ordinates at certain specified stations, provided that the functions $(x-x')\,g(x')$ and $\dfrac{d}{dx'}\{(x-x')\,g(x')\}$ are finite and continuous throughout the range $0 \leqslant x' \leqslant 1$. Equation (A.9) of Ref. 9 gives

$$\frac{1}{\pi}\int_0^1 \left(\frac{dz}{dx'}\right)g(x')\,dx' = \sum_{\mu=1}^{N-1} s_{\mu\nu}^{(1)}(x_\mu - x_\nu)^2\left(\frac{dg(x')}{dx'}\right)_{x'=x_\mu} z(x_\mu). \tag{22}$$

The stations $x_\mu$ and $x_\nu$ are tabulated in Table 3 and the coefficients $s_{\mu\nu}^{(1)}$ are given in Ref. 7.

Equation (20) satisfies these conditions, but (21) does not, since $K(k^2)$ tends to infinity like $\ln\{4/\sqrt{(1-k^2)}\}$ as $k^2 \to 1$. There is thus a singularity of the type $-\ln|x-x'|$, in the function $g(x')$ for equation (21). To deal with this, the integral may be written:

$$I = \frac{1}{\pi}\int_0^1 \left(\frac{dz}{dx'}\right)\left\{\frac{K(k^2)-E(k^2)}{\sqrt{\{(x-x')^2+4R^2\}}} + \ln|x-x'|\right\}dx'$$

$$-\frac{1}{\pi}\int_0^1 \left(\frac{dz}{dx'}\right)\ln|x-x'|\,dx'. \tag{23}$$

Integrating the second term by parts gives

$$\int_0^1 \left(\frac{dz}{dx'}\right) \ln |x - x'| \, dx' = \left[z(x') \ln |x - x'|\right]_0^1 + \int_0^1 \frac{z(x')}{x - x'} \, dx' \tag{24}$$

and, since $z(0) = z(1) = 0$, the first term here is zero.

An approximate form for the second term in (24) is given in equation (A.5) of Ref. 9:

$$\frac{1}{\pi} \int_0^1 \frac{z(x')}{x_\nu - x'} \, dx' = \sum_{\mu=1}^{N-1} s_{\mu\nu}^{(1)} (x_\mu - x_\nu) z(x_\mu) \, . \tag{25}$$

The first integral in equation (23) satisfies the necessary conditions for the approximation (22) to be valid, so that

$$\frac{1}{\pi} \int_0^1 \left(\frac{dz}{dx'}\right) \left\{ \frac{K(k^2) - E(k^2)}{\sqrt{\{(x - x')^2 + 4R^2\}}} + \ln |x - x'| \right\} dx'$$

$$= \sum s_{\mu\nu}^{(1)} (x_\mu - x_\nu)^2 \frac{d}{dx'} \left( \frac{K - E}{\sqrt{\{(x - x')^2 + 4R^2\}}} \right) z(x_\mu) + \sum s_{\mu\nu}^{(1)} (x_\mu - x_\nu) z(x_\mu) \, . \tag{26}$$

From equations (23), (25) and (26), therefore,

$$I = \sum s_{\mu\nu}^{(1)} (x_\mu - x_\nu)^2 \frac{d}{dx'} \left( \frac{K - E}{\sqrt{\{(x - x')^2 + 4R^2\}}} \right) z(x_\mu) \, .$$

The approximation (22) can be applied immediately to equation (20) but it is convenient to write the axial velocity increment as

$$v_{qx} = \bar{v}_{qx} + \Delta v_{qx} \, ,$$

where

$$\bar{v}_{qx} = \frac{1}{\pi} \int_0^1 \left(\frac{dz_t}{dx'}\right) \frac{dx'}{x - x'} = \sum_{\mu=1}^{N-1} s_{\mu\nu}^{(1)} z_t(x_\mu)$$

is the streamwise velocity increment produced by the two-dimensional aerofoil with the same thickness distribution.

The expressions finally obtained for the velocity increments due to the distribution of sources on a cylinder are therefore

$$\frac{v_{qx}(x_\nu, R)}{V_0} = \sum_{\mu=1}^{N-1} (s_{\mu\nu}^{(1)} + s_{\mu\nu}^{(27)}) \, z_t(x_\mu)$$

where

$$s_{\mu\nu}^{(27)} = s_{\mu\nu}^{(1)} \left\{ \frac{2R \{[3(x_\nu - x_\mu)^2 + 4R^2] E(k^2) - (x_\nu - x_\mu)^2 K(k^2)\}}{\{(x_\nu - x_\mu)^2 + 4R^2\}^{3/2}} - 1 \right\} \tag{27}$$

and

$$\frac{v_{qr}(x_\nu, R)}{V_0} = \pm \left(\frac{dz_t}{dx}\right)_{x_\nu} + \sum_{\mu=1}^{N-1} s_{\mu\nu}^{(28)} z_t(x_\mu)$$

where

$$s_{\mu\nu}^{(28)} = s_{\mu\nu}^{(1)} \frac{(x_\nu - x_\mu)\{(x_\nu - x_\mu)^2 K(k^2) + (4R^2 - (x_\nu - x_\mu)^2)E(k^2)\}}{\{(x_\nu - x_\mu)^2 + 4R^2\}^{3/2}}, \tag{28}$$

with

$$k^2 = \frac{4R^2}{(x_\nu - x_\mu)^2 + 4R^2}.$$

Values of the coefficients $s_{\mu\nu}^{(27)}$ and $s_{\mu\nu}^{(28)}$, for $N = 8$, have been calculated from equations (27) and (28) for the cases $R = \frac{1}{2}$ and $R = 1$; the results are given in Tables 1 and 2.

## APPENDIX II

### *The Axial Velocity Field of Certain Vortex Distributions*

The vortex distributions considered are of the form $\gamma(x, \varphi) = \gamma(x) \cos \varphi$, distributed along a cylinder of unit length and radius $R$. Trailing vortex elements of strength $1/R \cdot d\gamma/d\varphi$ will also be present, stretching along the cylinder, but these do not contribute to the axial velocity component.

By application of the Biot-Savart law, the axial velocity induced at a point $(x, r, \varphi)$ by a vortex distribution of strength $\Gamma \cos \varphi$ on a circle of radius $R$ in the plane $x = 0$ can be shown to be*

$$v_x = -\frac{\Gamma}{4\pi} \int_0^{2\pi} \frac{R(r \cos(\varphi - \varphi') - R) \cos \varphi'}{\{x^2 + r^2 + R^2 - 2rR \cos(\varphi - \varphi')\}^{3/2}} \, d\varphi' \,. \tag{29}$$

Writing $a^2$ for $(x^2 + r^2 + R^2)$, putting $\theta = \varphi - \varphi'$ and noting that

$$\int_0^{2\pi} \frac{\sin \theta}{(a^2 - 2rR \cos \theta)^{3/2}} \, d\theta = 0 \,,$$

equation (29) can be reduced to the form

$$v_x = -\frac{\Gamma}{4\pi} \, R \cos \varphi \left\{ r \int_0^{\pi} \frac{d\theta}{(a^2 - 2rR \cos \theta)^{3/2}} - 2R \int_0^{\pi} \frac{\cos \theta \, d\theta}{(a^2 - 2rR \cos \theta)^{3/2}} + \right.$$
$$\left. + \, r \int_0^{\pi} \frac{\cos 2\theta \, d\theta}{(a^2 - 2rR \cos \theta)^{3/2}} \right\} . \tag{30}$$

Each of the integrals in this expression can be reduced, by writing $\theta = \pi - 2\psi$, to the form

$$\frac{2}{\{x^2 + (r + R)^2\}^{3/2}} \int_0^{\pi/2} \frac{\cos 2n\psi}{(1 - k^2 \sin^2 \psi)^{3/2}} \, d\psi$$

with

$$k^2 = \frac{4rR}{x^2 + (r + R)^2} \,.$$

These integrals have been treated by Riegels[8], who has defined them as

$$G_n(k^2) = (-1)^n \int_0^{\pi/2} \frac{\cos 2n\psi}{(1 - k^2 \sin^2 \psi)^{3/2}} \, d\psi$$

and has evaluated them in terms of the complete elliptic integrals $E(k^2)$ and $K(k^2)$. Values of the functions $(1 - k^2)G_n(k^2)$ are tabulated in Refs. 8 and 8A.

Using Riegel's functions $G_n(k^2)$, equation (30) becomes

$$v_x = -\frac{\Gamma}{4\pi} \frac{2R \cos \varphi}{\{x^2 + (r + R)^2\}^{3/2}} \{rG_0(k^2) + rG_2(k^2) - 2RG_1(k^2)\} \,. \tag{31}$$

---

* The corresponding expression for the vortex ring of constant strength is derived in Ref. 1. The negative sign in equation (29) arises from the use of the same sign convention for positive vortex strength as in Ref. 1 (*see* footnote to Section 3).

The axial velocities induced by vortex distributions along a cylinder of unit length are now required. These velocities are of the form

$$v_x^{**}(x) \pm \frac{\gamma(x)}{2V_0},$$

where the second term represents the effect of the vortex ring at the point $x$, and the first term represents the integrated effect of the remainder of the vortices.

The first term can be evaluated by replacing $\Gamma$ by $\gamma(x')\,dx'$ and $x$ by $(x - x')$ in equation (31), and integrating over the range $0 \leqslant x' \leqslant 1$. Thus for points on the cylinder, $r = R$, and

$$v_x^{**}(x) = -\frac{R^2 \cos\varphi}{2\pi} \int_0^1 \gamma(x') \frac{[G_0(k^2) + G_2(k^2) - 2G_1(k^2)]}{\{(x - x')^2 + 4R^2\}^{3/2}}\,dx' \tag{32}$$

with

$$k^2 = \frac{4R^2}{(x - x')^2 + 4R^2}.$$

For the present application, the velocity increments $v_{xm}^{**}(x)$ associated with the first three Birnbaum vortex distributions

$$\gamma_1(x) = 2\pi V_0 \sqrt{\left(\frac{1 - x}{x}\right)}$$

$$\gamma_2(x) = 2\pi V_0 \sqrt{\{1 - (1 - 2x)^2\}}$$

$$\gamma_3(x) = 2\pi V_0 (1 - 2x) \sqrt{\{1 - (1 - 2x)^2\}}$$

are required. To obtain them, equation (32) must be evaluated numerically, and this is not quite straightforward since the functions $G_n(k^2)$ tend to infinity as $k^2 \to 1$, i.e. at $x = x'$.

Using the asymptotic expressions given by Riegels for $G_n(k^2)$, for values of $k^2$ near 1,

$$G_0(k^2) + G_2(k^2) - 2G_1(k^2) = 12 + 26(1 - k^2) + 40\cdot219(1 - k^2)^2 + \ldots$$

$$- \ln \frac{4}{\sqrt{(1 - k^2)}} \{4 + 15(1 - k^2) + 25\cdot312(1 - k^2)^2 + \ldots\}. \tag{33}$$

Thus it appears that the integrand in equation (32) tends to infinity like $\ln(x - x')$. The integrals of (32) can therefore be obtained numerically by using the theorem

$$\int_0^{a^2} f(x)\,dx = 2\int_0^a f(x)\,\sqrt{x}\,d\sqrt{x},$$

since

$$x^{1/2} \ln x \to 0 \text{ as } x \to 0.$$

The appropriate transformation of equation (32) is

$$v_{xm}^{**}(x) = -\frac{R^2}{2\pi} \cos\varphi \left[2\int_0^{\sqrt{(1-x)}} \gamma_m(x')\,p(x - x')\,\sqrt{(x' - x)}\,d\sqrt{(x' - x)} + \right.$$

$$\left. + 2\int_0^{\sqrt{x}} \gamma_m(x')\,p(x - x')\sqrt{(x - x')}\,d\sqrt{(x - x')}\right], \tag{34}$$

where

$$p(x - x') = \frac{G_0(k^2) + G_2(k^2) - 2G_1(k^2)}{\{(x - x')^2 + 4R^2\}^{3/2}} .$$

The expression (34) can be conveniently used, except for the point $x = 0$ and the vortex distribution $\gamma_1(x)$, where the integrand in equation (33) tends to infinity like $(\ln x)/\sqrt{x}$. This can be reduced to a form with finite integrand by using the relation

$$\int_0^{b^4} f(x)\, dx = 4 \int_0^b f(x)\, x^{3/4}\, d(x^{1/4}) .$$

In evaluating the integrand in equation (34), the formula (33) was used to obtain values of $\{G_0(k^2) + G_2(k^2) - 2G_1(k^2)\}$ for values of $k^2$ not tabulated by Riegels.

The calculations have been made only for the case $R = 1$. The results are given in Table 4.

TABLE 1

*Values of the Coefficients* $s_{\mu\nu}^{(27)}$ *for Equation* (7)

$R = 1$

| $\mu$ \ $\nu$ | 1 | 2 | 3 | 4 | 5 | 6 | 7 | 8 |
|---|---|---|---|---|---|---|---|---|
| 1 | 0 | +0·0111 | 0 | +0·0010 | 0 | −0·0026 | 0 | −0·0032 |
| 2 | +0·0205 | 0 | +0·0153 | 0 | −0·0003 | 0 | −0·0047 | 0 |
| 3 | 0 | +0·0200 | 0 | +0·0174 | 0 | −0·0004 | 0 | −0·0025 |
| 4 | +0·0027 | 0 | +0·0188 | 0 | +0·0188 | 0 | +0·0027 | 0 |
| 5 | 0 | −0·0004 | 0 | +0·0174 | 0 | +0·0200 | 0 | +0·0091 |
| 6 | −0·0047 | 0 | −0·0003 | 0 | +0·0153 | 0 | +0·0205 | 0 |
| 7 | 0 | −0·0026 | 0 | +0·0010 | 0 | +0·0111 | 0 | +0·0054 |

$R = \frac{1}{2}$

| $\mu$ \ $\nu$ | 1 | 2 | 3 | 4 | 5 | 6 | 7 | 8 |
|---|---|---|---|---|---|---|---|---|
| 1 | 0 | +0·0238 | 0 | −0·0126 | 0 | −0·0148 | 0 | −0·0149 |
| 2 | +0·0441 | 0 | +0·0256 | 0 | −0·0273 | 0 | −0·0274 | 0 |
| 3 | 0 | +0·0334 | 0 | +0·0220 | 0 | −0·0356 | 0 | −0·0381 |
| 4 | −0·0328 | 0 | +0·0238 | 0 | +0·0238 | 0 | −0·0328 | 0 |
| 5 | 0 | −0·0356 | 0 | +0·0220 | 0 | +0·0334 | 0 | −0·1253 |
| 6 | −0·0274 | 0 | −0·0273 | 0 | +0·0256 | 0 | +0·0441 | 0 |
| 7 | 0 | −0·0148 | 0 | −0·0126 | 0 | +0·0238 | 0 | −0·0061 |

TABLE 2

*Values of the Coefficients* $s_{\mu\nu}^{(28)}$ *for Equation* (8)

$R = 1$

| $\mu$ \ $\nu$ | 1 | 2 | 3 | 4 | 5 | 6 | 7 | 8 |
|---|---|---|---|---|---|---|---|---|
| 1 | 0 | +0·2229 | 0 | +0·0555 | 0 | +0·0315 | 0 | +0·0271 |
| 2 | −0·4118 | 0 | +0·2780 | 0 | +0·0877 | 0 | +0·0581 | 0 |
| 3 | 0 | −0·3633 | 0 | +0·3094 | 0 | +0·1145 | 0 | +0·0905 |
| 4 | −0·1451 | 0 | −0·3349 | 0 | +0·3349 | 0 | +0·1451 | 0 |
| 5 | 0 | −0·1145 | 0 | −0·3094 | 0 | +0·3633 | 0 | +0·1961 |
| 6 | −0·0581 | 0 | −0·0877 | 0 | −0·2780 | 0 | +0·4118 | 0 |
| 7 | 0 | −0·0315 | 0 | −0·0555 | 0 | −0·2229 | 0 | +0·6298 |

TABLE 2—*continued*

$R = \frac{1}{2}$

| $\nu$ / $\mu$ | 1 | 2 | 3 | 4 | 5 | 6 | 7 | 8 |
|---|---|---|---|---|---|---|---|---|
| 1 | 0 | +0·4545 | 0 | +0·1090 | 0 | +0·0473 | 0 | +0·0660 |
| 2 | −0·8399 | 0 | +0·5731 | 0 | +0·1642 | 0 | +0·0874 | 0 |
| 3 | 0 | −0·7488 | 0 | +0·6404 | 0 | +0·2144 | 0 | +0·2005 |
| 4 | −0·2852 | 0 | −0·6932 | 0 | +0·6932 | 0 | +0·2852 | 0 |
| 5 | 0 | −0·2144 | 0 | −0·6404 | 0 | +0·7488 | 0 | +0·4053 |
| 6 | −0·0874 | 0 | −0·1642 | 0 | −0·5731 | 0 | +0·8399 | 0 |
| 7 | 0 | −0·0473 | 0 | −0·1090 | 0 | −0·4545 | 0 | +1·2660 |

TABLE 3

*Positions of the Pivotal Points $x_\mu$, $x_\nu$ for $N = 8$*

| $\mu$ or $\nu$ | $x_\mu$ or $x_\nu$ |
|---|---|
| 1 | 0·9619 |
| 2 | 0·8536 |
| 3 | 0·6913 |
| 4 | 0·5000 |
| 5 | 0·3087 |
| 6 | 0·1464 |
| 7 | 0·0381 |

TABLE 4

*Axial Velocity Increments Due to First Three Standard Vortex Distributions from Equation* (32)

$R = 1$

| $x$ | $v^{**}_{x_1}$ | $v^{**}_{x_2}$ | $v^{**}_{x_3}$ |
|---|---|---|---|
| 0 | 1·25 | 0·108 | +0·091 |
| 0·1 | 1·05 | 0·219 | 0·145 |
| 0·2 | 0·88 | 0·307 | 0·148 |
| 0·3 | 0·73 | 0·367 | 0·117 |
| 0·4 | 0·60 | 0·404 | +0·066 |
| 0·5 | 0·49 | 0·416 | 0 |
| 0·6 | 0·38 | 0·404 | −0·066 |
| 0·7 | 0·28 | 0·367 | −0·117 |
| 0·8 | 0·18 | 0·307 | −0·148 |
| 0·9 | 0·09 | 0·219 | −0·145 |
| 1·0 | 0 | 0·108 | −0·091 |

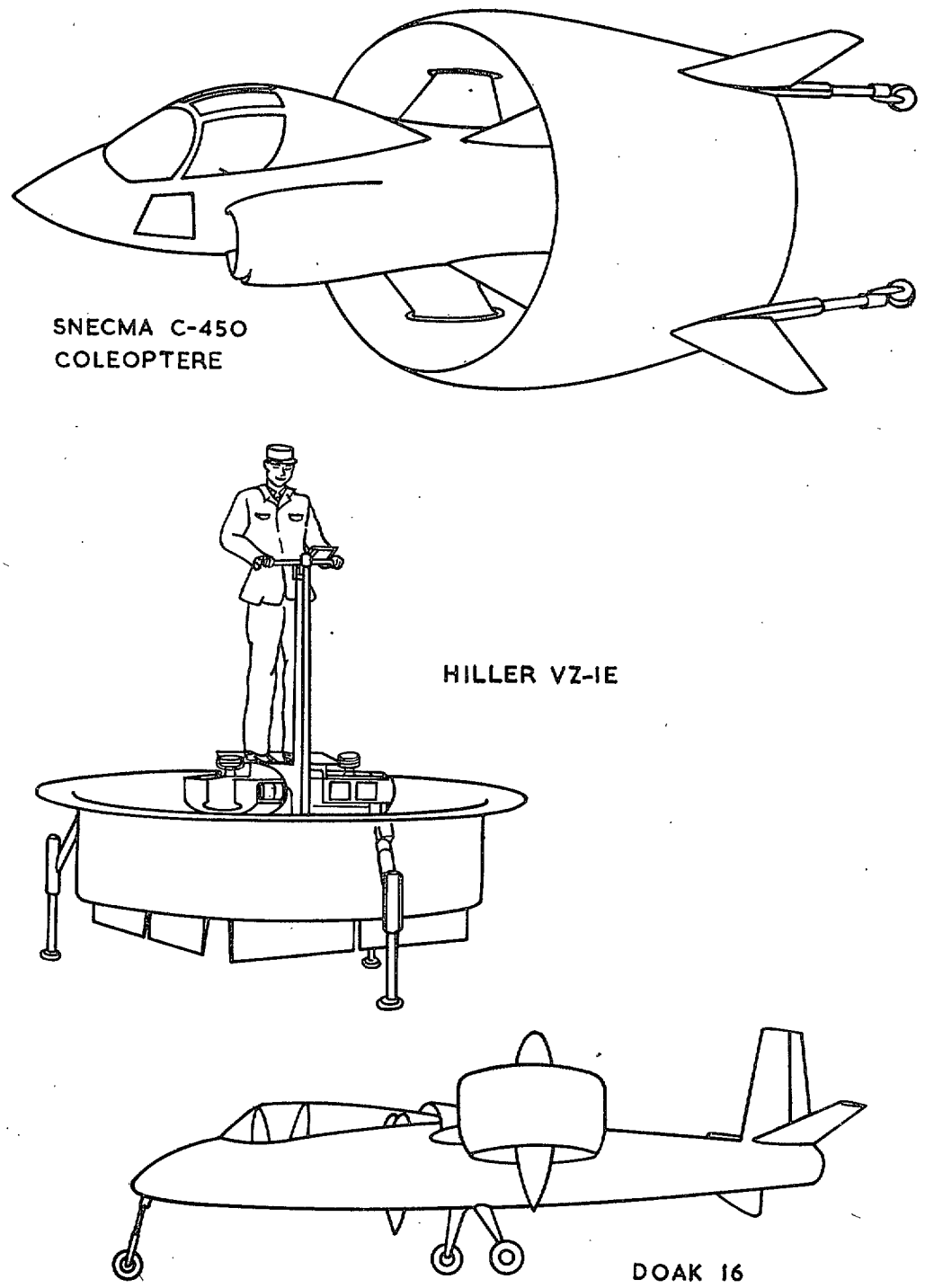


FIG. 1. Some aircraft configurations utilising annular wings.

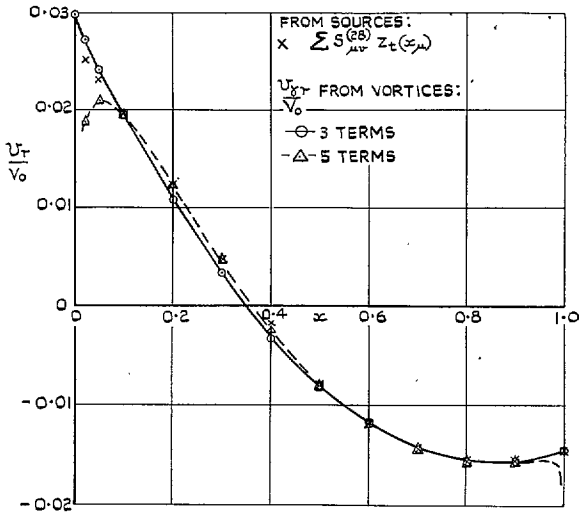


R.A.E 101 – 10% SECTION; R = 1.

FIG. 2. Radial velocity distribution due to source and vortex distributions.

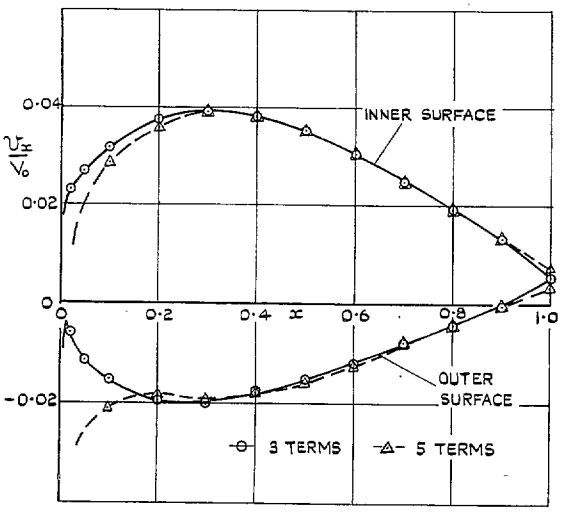


R.A.E. 101 – 10% SECTION; R = 1

FIG. 3. Axial velocity distribution due to vortex distribution.

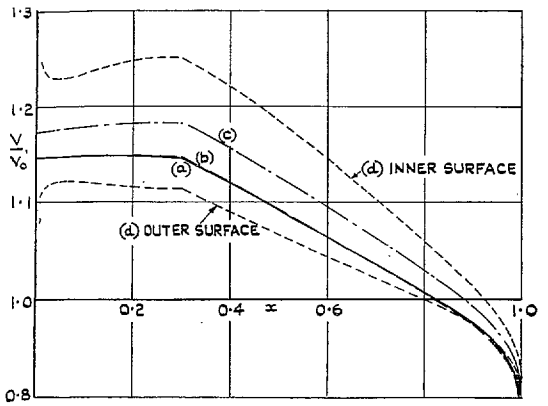


R.A.E. 101 – 10%; R = ½

(a) ——— $V/V_0 = 1 + S^{(1)}(x)$

(b) — — $V/V_0 = 1 + S^{(1)}(x) + S^{(2\eta)}(x)$

(c) —·— $V/V_0 = 1 + S^{(1)}(x) + S^{(2\eta)}(x) + \Sigma C_m v^*_{x_m}$

(d) ----- $V/V_0 = 1 + S^{(1)}(x) + S^{(2\eta)}(x) + \Sigma C_m v^*_{x_m} \pm \Sigma C_m \frac{\gamma_m}{2V_0}$

FIG. 4. Contribution of various terms to velocity distribution.

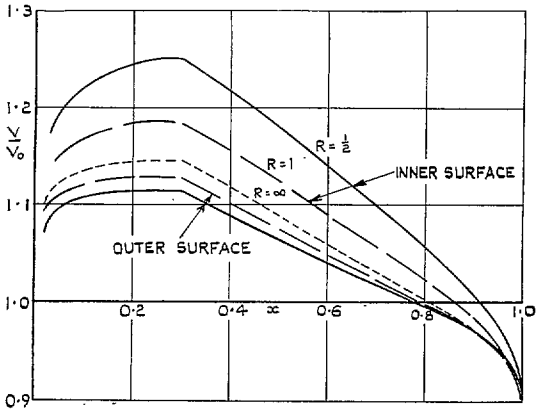


$$\frac{V}{V_0} = \frac{1 + S^{(1)}(x) + S^{(2\eta)}(x) + \Sigma C_m v^*_{x_m} \pm \Sigma C_m \frac{\gamma_m}{2V_0}}{\sqrt{1 + \left(\frac{dz}{dx}\right)^2}}$$

R.A.E. 101 = 10% SECTIONS

——— R = ½

—·— R = 1

----- R = ∞

FIG. 5. Calculated velocity distribution on annular and two-dimensional aerofoils at zero incidence.

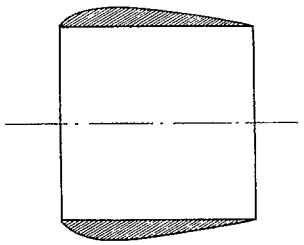

(a) SKETCH OF AEROFOIL R = 1/2
10% R.A.E. 101 WITH 5% R.A.E. 101 CAMBER LINE.

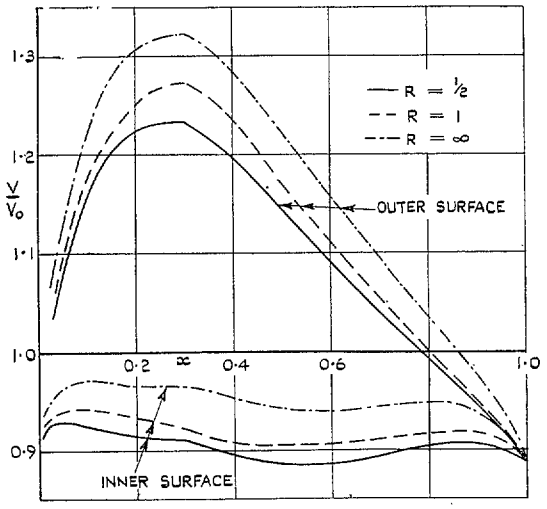


(b) CALCULATED VELOCITY DISTRIBUTIONS.
10% R.A.E. 101, WITH 5% R.A.E. 101 CAMBER.

FIGS. 6a and 6b. Velocity distribution on cambered annular aerofoils at zero incidence.

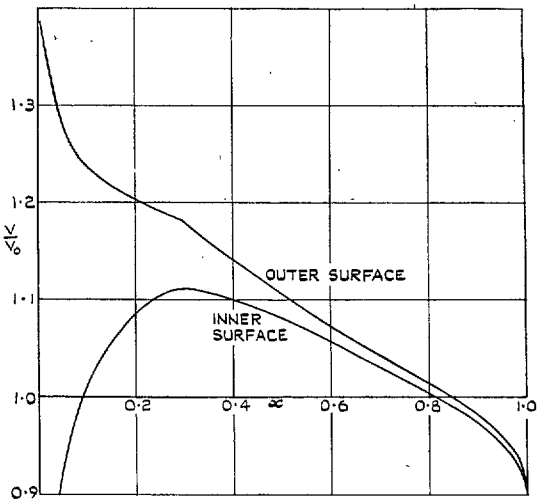


(a) TOP OF AEROFOIL ($\varphi = 0$)

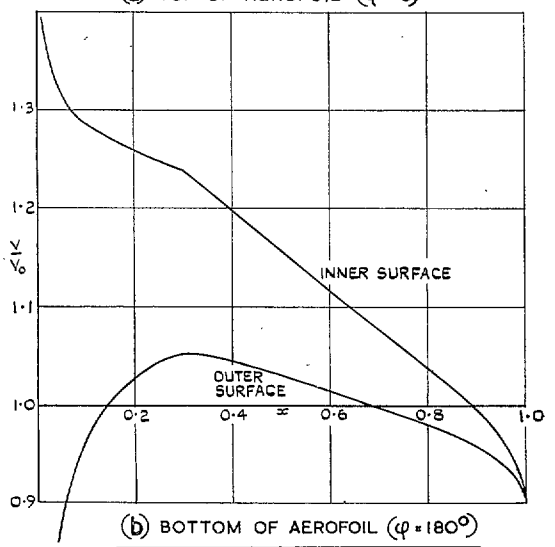


(b) BOTTOM OF AEROFOIL ($\varphi = 180°$)

R.A.E. 101 – 10% SECTION; R = 1

FIGS. 7a and 7b. Calculated velocity distributions on annular aerofoil at 5 deg incidence.



(78681) Wt. 54/8210 3/61 K.5 Hw

# Publications of the Aeronautical Research Council

## ANNUAL TECHNICAL REPORTS OF THE AERONAUTICAL RESEARCH COUNCIL (BOUND VOLUMES)

1941 Aero and Hydrodynamics, Aerofoils, Airscrews, Engines, Flutter, Stability and Control, Structures. 63*s.* (post 2*s.* 3*d.*)

1942 Vol. I. Aero and Hydrodynamics, Aerofoils, Airscrews, Engines. 75*s.* (post 2*s.* 3*d.*)
Vol. II. Noise, Parachutes, Stability and Control, Structures, Vibration, Wind Tunnels. 47*s.* 6*d.* (post 1*s.* 9*d.*)

1943 Vol. I. Aerodynamics, Aerofoils, Airscrews. 80*s.* (post 2*s.*)
Vol. II. Engines, Flutter, Materials, Parachutes, Performance, Stability and Control, Structures. 90*s.* (post 2*s.* 3*d.*)

1944 Vol. I. Aero and Hydrodynamics, Aerofoils, Aircraft, Airscrews, Controls. 84*s.* (post 2*s.* 6*d.*)
Vol. II. Flutter and Vibration, Materials, Miscellaneous, Navigation, Parachutes, Performance, Plates and Panels, Stability, Structures, Test Equipment, Wind Tunnels. 84*s.* (post 2*s.* 6*d.*)

1945 Vol. I. Aero and Hydrodynamics, Aerofoils. 130*s.* (post 3*s.*)
Vol. II. Aircraft, Airscrews, Controls. 130*s.* (post 3*s.*)
Vol. III. Flutter and Vibration, Instruments, Miscellaneous, Parachutes, Plates and Panels, Propulsion. 130*s.* (post 2*s.* 9*d.*)
Vol. IV. Stability, Structures, Wind Tunnels, Wind Tunnel Technique. 130*s.* (post 2*s.* 9*d.*)

1946 Vol. I. Accidents, Aerodynamics, Aerofoils and Hydrofoils. 168*s.* (post 3*s.* 3*d.*)
Vol. II. Airscrews, Cabin Cooling, Chemical Hazards, Controls, Flames, Flutter, Helicopters, Instruments and Instrumentation, Interference, Jets, Miscellaneous, Parachutes. 168*s.* (post 2*s.* 9*d.*)
Vol. III. Performance, Propulsion, Seaplanes, Stability, Structures, Wind Tunnels. 168*s.* (post 3*s.*)

1947 Vol. I. Aerodynamics, Aerofoils, Aircraft. 168*s.* (post 3*s.* 3*d.*)
Vol. II. Airscrews and Rotors, Controls, Flutter, Materials, Miscellaneous, Parachutes, Propulsion, Seaplanes, Stability, Structures, Take-off and Landing. 168*s.* (post 3*s.* 3*d.*)

## Special Volumes

Vol. I. Aero and Hydrodynamics, Aerofoils, Controls, Flutter, Kites, Parachutes, Performance, Propulsion, Stability. 126*s.* (post 2*s.* 6*d.*)
Vol. II. Aero and Hydrodynamics, Aerofoils, Airscrews, Controls, Flutter, Materials, Miscellaneous, Parachutes, Propulsion, Stability, Structures. 147*s.* (post 2*s.* 6*d.*)
Vol. III. Aero and Hydrodynamics, Aerofoils, Airscrews, Controls, Flutter, Kites, Miscellaneous, Parachutes, Propulsion, Seaplanes, Stability, Structures, Test Equipment. 189*s.* (post 3*s.* 3*d.*)

## Reviews of the Aeronautical Research Council

1939–48 3*s.* (post 5*d.*) 1949–54 5*s.* (post 5*d.*)

## Index to all Reports and Memoranda published in the Annual Technical Reports

1909–1947 R. & M. 2600 6*s.* (post 2*d.*)

## Indexes to the Reports and Memoranda of the Aeronautical Research Council

| | |
|---|---|
| Between Nos. 2351–2449 | R. & M. No. 2450 2*s.* (post 2*d.*) |
| Between Nos. 2451–2549 | R. & M. No. 2550 2*s.* 6*d.* (post 2*d.*) |
| Between Nos. 2551–2649 | R. & M. No. 2650 2*s.* 6*d.* (post 2*d.*) |
| Between Nos. 2651–2749 | R. & M. No. 2750 2*s.* 6*d.* (post 2*d.*) |
| Between Nos. 2751–2849 | R. & M. No. 2850 2*s.* 6*d.* (post 2*d.*) |
| Between Nos. 2851–2949 | R. & M. No. 2950 3*s.* (post 2*d.*) |
| Between Nos. 2951–3049 | R. & M. No. 3050 3*s.* 6*d.* (post 2*d.*) |

HER MAJESTY'S STATIONERY OFFICE

*from the addresses overleaf*

Printed and published by
HER MAJESTY'S STATIONERY OFFICE

To be purchased from
York House, Kingsway, London W.C.2
423 Oxford Street, London W.1
13A Castle Street, Edinburgh 2
109 St. Mary Street, Cardiff
39 King Street, Manchester 2
50 Fairfax Street, Bristol 1
2 Edmund Street, Birmingham 3
80 Chichester Street, Belfast 1
or through any bookseller

*Printed in England*



S.O. Code No. 23-3146